2021. Journal of Arachnology 49:235–249

Elemental enrichment of the exoskeleton of the whip spider *Phrynus marginemaculatus* (Arachnida: Amblypygi)

Dragoslav Radosavljevic, Earl Ada and **Rick Hochberg**: University of Massachusetts Lowell, One University Avenue, Lowell MA 01854; E-mail: Rick_Hochberg@uml.edu

Abstract. Amblypygi is a small order of arachnids that includes the whip spiders. Like other members of the clade Pedipalpi, these arachnids are cryptic predators that use their antenniform appendages to detect prey, and spinose pedipalps for quick prey capture. To date, there is very little information on the composition of their exoskeleton despite its importance in predation and defense. Here, we performed the first analysis of a whip spider exoskeleton using energy-dispersive X-ray spectroscopy (SEM-EDS). Our studies of *Phrynus marginemaculatus* CL Koch, 1840 were designed to (1) determine if elemental profiles differ between instars and (2) determine if and how elemental profiles of whip spiders differ from other closely related arachnids. We found the whip spider exoskeleton to contain several trace metal elements including calcium, magnesium, manganese, potassium, sodium, and zinc. The diversity and abundance of trace elements is relatively low throughout the exoskeleton of 2nd instars but increases in adults. In particular, the chelicerae and pedipalps are well reinforced with several metal elements, most notably calcium and zinc, which are also present in the tarsal claws. A similar elemental distribution is known for adult whip scorpions (Thelyphonida). In *P. marginemaculatus*, these metal elements are similarly present in adult exuviae. The elemental enrichment of the whip spider exoskeleton is comparable to that present in other members of the Pedipalpi and Tetrapulmonata, reflecting a relatively conserved profile for the few species that have been examined.

Keywords: Transition metals, chelicerate, enrichment, whip spiders, SEM-EDS

https://doi.org/10.1636/JoA-S-20-048

Amblypygi is a relatively small order of Arachnida with little more than 200 species commonly referred to as whip spiders, which are mostly epigean predators of terrestrial insects (Chapin & Hebets 2016; Miranda et al. 2016). Their body shape is reminiscent of true spiders (Araneae) with the exceptions of being dorsoventrally flattened, possessing raptorial pedipalps, and having an elongate first pair of walking legs (antenniform) that function in tactile and olfactory sensation (Weygoldt 2000); the latter characteristic is shared with species of Schizomida and Thelyphonida, together forming the clade Pedipalpi (Scholtz & Kamenz 2006; Shultz 2007; Dunlop 2010; Sharma et al. 2014; Lehmann & Melzer 2019; Nolan et al. 2020). Whip spiders live in tropical and subtropical regions of the world, where they inhabit a large variety of ecological niches from deserts and caves to tropical rainforests (Weygoldt 2000; Chapin & Hebets 2016). Species that live in semi-xeric and xeric conditions in savannahs and deserts are considered living relicts that have adapted to new conditions after the disappearance of rainforests (Weygoldt 2000).

Whip spiders are predominantly nocturnal opportunistic predators that feed on other arthropods (Weygoldt 2000; Chapin & Hebets 2016). As small to large-sized raptorial arachnids, whip spiders are extremely agile and adapted for quick predatory strikes on mobile prey, most of which are insects (Weygoldt 2000; Hebets 2002; Chapin & Hebets 2016), though some whip spiders are known to feed on harvestmen (Hebets 2002), millipedes (Hebets 2002), scorpions (Forcellado & Armas 2014; Chapin & Hebets 2016), spiders (Hebets 2002), freshwater prawns (Ladle & Velander 2003), lizards (Reagan 1996; Kok 1998), and even hummingbirds (Owen & Cokendolpher 2006). Based on limited observations, whip spiders appear to engage in fairly stereotyped predatory behaviors that include an initial positioning of their body towards the prey, spreading their antenniform legs on either side of the prey (presumably for chemosensation), extending their chelicerae and pedipalps in a pre-strike orientation, and then quickly lunging towards the prey to grasp it between the pedipalps (Santer & Hebets 2009a; Seiter et al. 2019; Segovia et al. 2020). These movements ensure that the whip spider's dominant weaponry—an array of exoskeletal spines on the medial and distal surfaces of the pedipalps—contact the prey before any vulnerable regions (e.g., walking legs, main body) become exposed. It also guarantees that the chelicerae, which themselves bear dentition, have unimpeded access to the prey for piercing, chewing and tearing. Importantly, whip spiders do not possess chelate appendages that can hold prey at a distance and slowly tear them apart (e.g., as in scorpions), nor do they possess any venom glands that can immobilize prey (e.g., as in spiders and scorpions). Therefore, it is imperative that the spines and dentition of their appendages be strong enough to immobilize and even penetrate the prey, which itself might be armored with an exoskeleton. To date, most of the data on these spines is limited to their general morphology, orientation, and in some cases, surface ultrastructure, all of which can be important for taxonomy (Weygoldt 2000). There is no data on the ultrastructure of the cuticle in these regions, nor is it known if the elemental composition of these exoskeletal elaborations differs in any significant way from the rest of the body, as might be expected for such weaponry (Schofield 2001).

To date, there is limited information on the structure of the amblypygid exoskeleton that might provide insights into their ecology and evolution. The most detailed studies come from analyses of the cerotegument, a structurally diverse hydrophobic layer on top of the epicuticle that may aid in self-

cleaning, plastron respiration, and/or inhibition of bacterial growth (Wolff et al. 2016a, b; Filipov et al. 2017). There are no chemical or ultrastructural studies of the laminae that constitute the exoskeleton—unlike for many other arachnids (e.g., Krishnakumaran 1961, 1962)—and the only study of its elemental profile comes from observations by Schofield (2001), who found manganese and zinc in the chelicerae and pedipalps of an unidentified specimen. According to Cutler & McCutchen (2006), these two elements are characteristic of the exoskeleton of many species of arachnids from several orders (e.g., Araneae, Pseudoscorpiones, Scorpiones, Solifugae). While the precise functions of these metal elements remain to be determined, enrichment with zinc is proposed to add hardness to the exoskeleton, which explains why it is often found in the distal regions of appendages that function in predation (e.g., chelicerae, pedipalps) and defense (e.g., pedipalps) (Gallant et al. 2016). Arachnids from other orders also possess zinc in their appendages (e.g., Palpigradi, Schizomida, Thelyphonida); while manganese is never present, additional elements such as halogens and alkaline earth metal elements can be present (Schofield & Levere 1989; Schofield et al. 1989, 2003; Schofield 1990; Cutler & McCutchen 2006; Politi et al. 2012; Gallant et al. 2016; Gallant & Hochberg 2017; Tadayon et al. 2020). These data suggest that there is some phylogenetic conservation in the metal ion enrichment of the exoskeleton of arachnids, but too few species outside of Scorpiones (Schofield 2001) have been examined to make any conclusions.

Here, we used scanning electron microscopy-energy dispersive X-ray spectroscopy (SEM-EDS) to study the amblypygid, *Phrynus marginemaculatus* CL Koch, 1840. This species has been the subject of tactile learning studies (Santer & Hebets 2009a), neuroanatomy (Spence & Hebets 2006), prey capture (Santer & Hebets 2009b), plastron respiration (Hebets & Chapman 2000; Wolff et al. 2016a), and territoriality (Fowler-Finn & Hebets 2006). We studied *P. marginemaculatus* to answer two basic questions:

(1) Does the exoskeleton of this species share a similar elemental profile to that of other arachnids, with particular emphasis on the exoskeleton of the appendages (e.g., chelicerae, pedipalps, leg tarsi) that are prone to abrasion?
(2) Are there detectable differences in elemental profiles among age groups (instars) raised in a similar environment?

METHODS

Live specimens of *Phrynus marginemaculatus* originating from Florida, USA were obtained from LLL Reptile and Supply Company, Inc. (California, USA). Species identity was confirmed with the key by Quintero Jr. (1981): two teeth on the external margin of the cheliceral basal article (Figs. 1c, 4c) and a shared common base for spines 1 and 2 on the ventral side of pedipalp femur. Specimens were kept in terrariums held at ~24 °C and fed with the house cricket *Acheta domesticus* (Linnaeus, 1758). A breeding colony was established to obtain 2nd instars (Fig. 1a). For SEM and EDS analyses, a total of four whip spiders (all captive-bred: one reproductive adult, three 2nd instars) were euthanized by putting each specimen in a small jar containing a chloroform-soaked cotton ball, followed by placement of the jar in a freezer (-20 °C) for 30 minutes. Euthanized specimens were dehydrated by immersion in 70% ethanol for 72 hours, and then transitioned to 100% ethanol in 10% increments for 10 minutes per solution. Specimens were then air dried in a desiccator for 24 hrs to remove all liquid from the tissues. Additionally, the complete molts of two adult specimens were examined after being maintained in a desiccator for 24 hrs.

Dry specimens and exuviae were dissected with forceps and fine dissection scissors under a Zeiss Stemi stereoscope. The following structures were removed: chelicerae, pedipalps, walking legs, antenniform appendages, and portions of the main body cuticle (prosoma). All structures were maintained in a desiccator until they were ready for mounting. Specimens were mounted using double-sided conductive carbon tape on top of carbon SEM specimen stubs (Ted Pella, Inc., USA). Specimens were coated with 12 nm of gold by using a Denton Vacuum Desk IV Sputter Coater. The coating was performed three times for 120 seconds with 25 % of full plasma discharge current. All microscopy and spectroscopy were carried out using a JEOL JSM 7401F Field Emission Scanning Electron Microscope (SEM) equipped with an EDAX energy dispersive X-ray spectrometer (EDS) located at the Core Research Facilities at the University of Massachusetts Lowell. Data were collected with the EDAX Genesis XM2 Imaging System Software, version 4.61. The following SEM imaging parameters were used: acceleration voltage of 5 kV, emission current of 10 μA, and a probe current setting of 9. The following EDS spectral acquisition parameters were used: acceleration voltage of 17 kV, emission current of 10 μA, a probe current setting of 14, X-ray collection live time of 100 s, and amp time of 102.4 μs.

Polishing of specimens to a flat surface is often recommended for EDS analyses to obtain accurate signals and collect quantifiable data (Newbury & Ritchie 2013). However, this can be difficult to perform on small appendages without damaging the cuticle, particularly the surface layers where transition metal elements may be present, which would bias the results. For this reason, none of our specimens were polished. While we do provide estimates of elemental composition (weight percentage), it is understood that such data are more appropriate for qualitative rather than quantitative, and hence statistical, comparisons.

Because the electron beam is thought to only penetrate through approximately 4 – 7 μm of the organic material (Dawes 1994; Chandler & Roberson 2009), the EDS data collected are only related to the uppermost layers of a whip spider's exoskeleton. Depending on the size and age of the specimen, the cuticle thickness was from 10 to 20 μm (based on SEM thickness measurements of a fractured cuticle), thus allowing the EDS electron beam to penetrate 30–70% into the cuticle. The body parts examined included prosoma (carapace), chelicerae (basal, distal article (fang), teeth); pedipalp (tibial base and spines, basitarsus and distitarsus) and the tarsal claws of the first pair of walking legs. Each area was scanned at least three times. The presence of zinc on any specimen was exclusively confirmed by the appearance of its Zn Kα peak at 8.637 keV. To quantify Na and Zn, which have

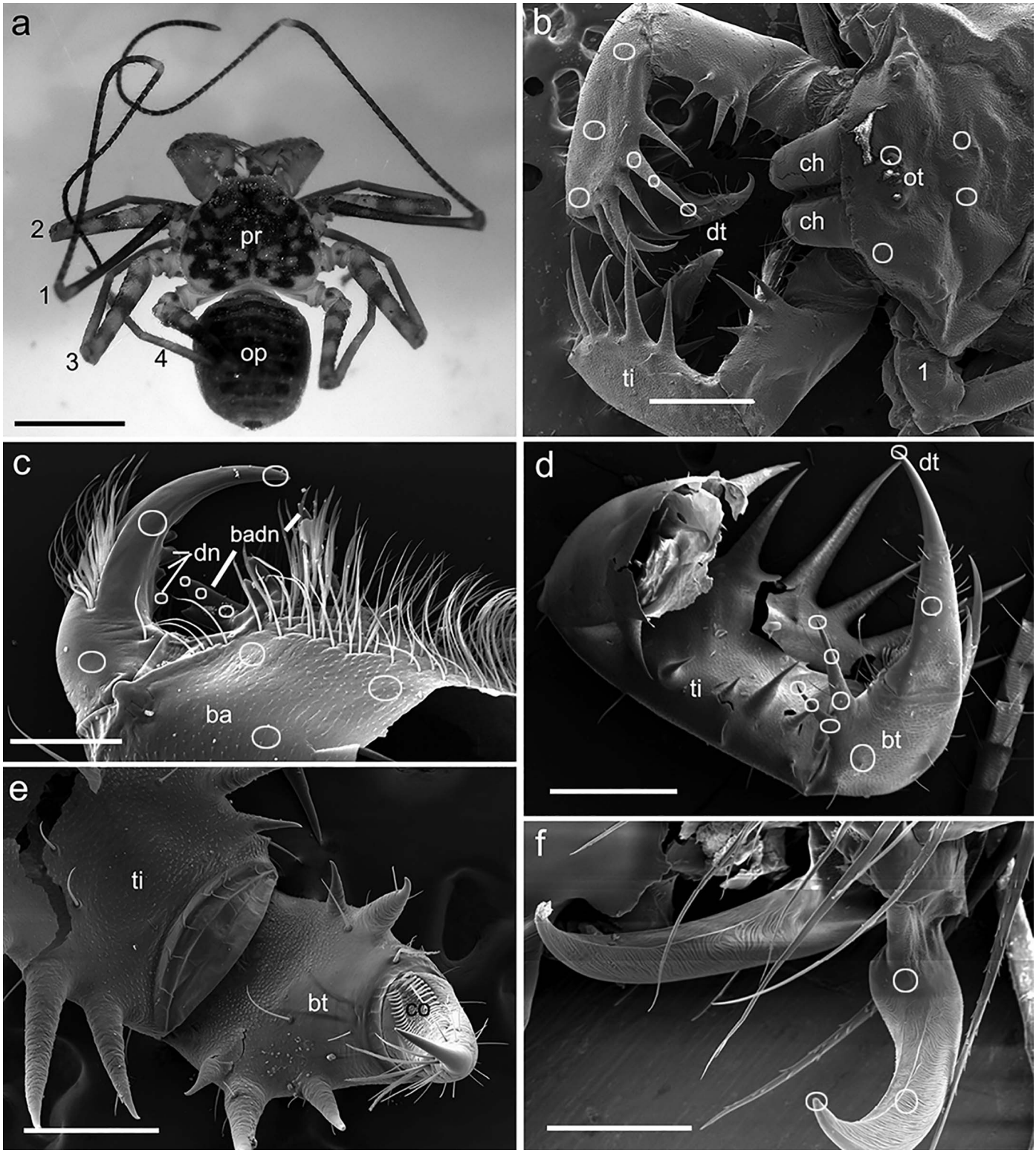

Figure 1.—Juvenile (2nd instar) *Phrynus maginemaculatus*. a. Dead specimen, dorsal view. b–e. Scanning electron micrographs of regions scanned for elemental enrichment. Ovals represent approximate regions of EDS data collection. See text for specific locations. b. Anterior end. c. Chelicera. d. Pedipalp. e. Pedipalp showing the cleaning organ. f. Tarsal claws. Abbreviations: 1–4, walking legs from anterior to posterior; ba, basal article of chelicera; badn, basal article dentition; bt, basitarsus of pedipalp; ch, chelicera from dorsal view showing basal article; co, cleaning organ; dn, dentition of chelicera; dt, distitarsus of pedipalp; op, opisthosoma; ot, ocular tubercle; pr, prosoma, ti, tibia of pedipalp. Scale bars: a, 1.5 mm; b, 500 μm; c, 200 μm; d, 500 μm; e, 300 μm; f, 100 μm.

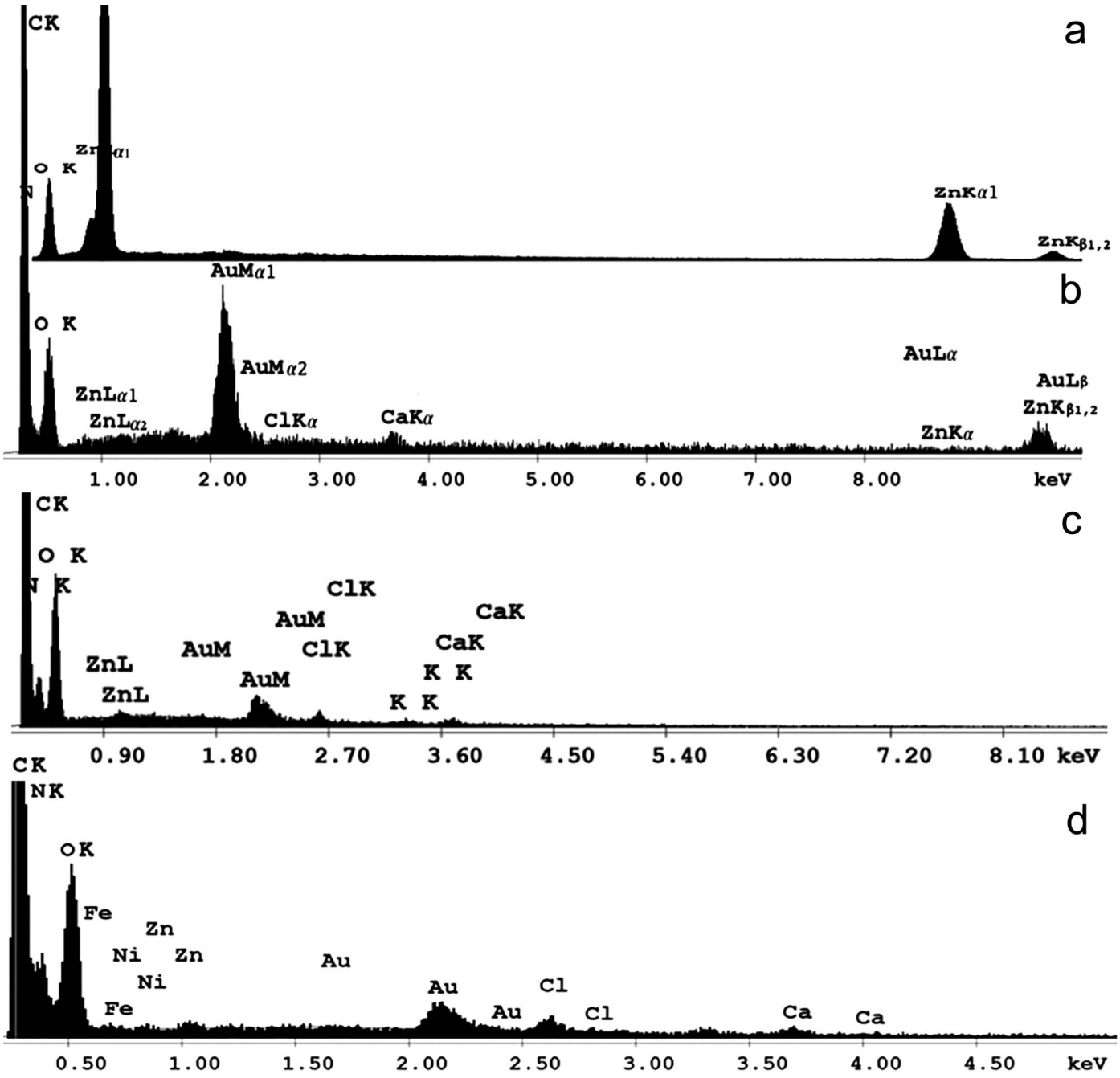

Figure 2.—EDS spectrograms of controls and exoskeleton of *Phrynus maginemaculatus*. a. EDS spectrum of zinc oxide powder as a control to help understand distinctions between shell energies of ZnLα (1.012 keV) and ZnKα (1.041 keV), and ZnKβ (8.630 keV) and AuLβ (9.712 keV), which tend to overlap. b. EDS spectrum of the pedipalp distitarsus seta of an adult *P. marginemaculatus* as a comparison to the control. X–axis represents excitation energy of the emitted X-rays (in keV); Y–axis represents the relative X-ray line intensities. c. Prosoma of juvenile, dorsal side. d. Chelicera of juvenile.

overlapping peaks i.e., similar energies on an EDS scan (Newbury 2009), we ran controls using zinc oxide (ZnO) powder to better understand how to separate NaK and ZnL shell energies and determine the relative amounts of each element (Fig. 2a, b). Ten control scans of ZnO powder were performed and ZnL/ZnK ratios with SD calculated – the average ZnL/ZnK ratio was 3.69 ± 0.99%. The controls allowed the confirmation of the presence or absence of zinc in relation to sodium. Whenever the ZnL/ZnK ratio in the specimen scans was higher than 4.70, that confirmed the presence of Na (the ZnL/ZnK ratio was never below 2.70). The elemental analyses were conducted with standardless quantification, aided by matrix corrections, that included stopping power corrections, backscattering electrons corrections, absorption attenuation corrections, and fluorescence corrections (Chandler & Roberson 2009).

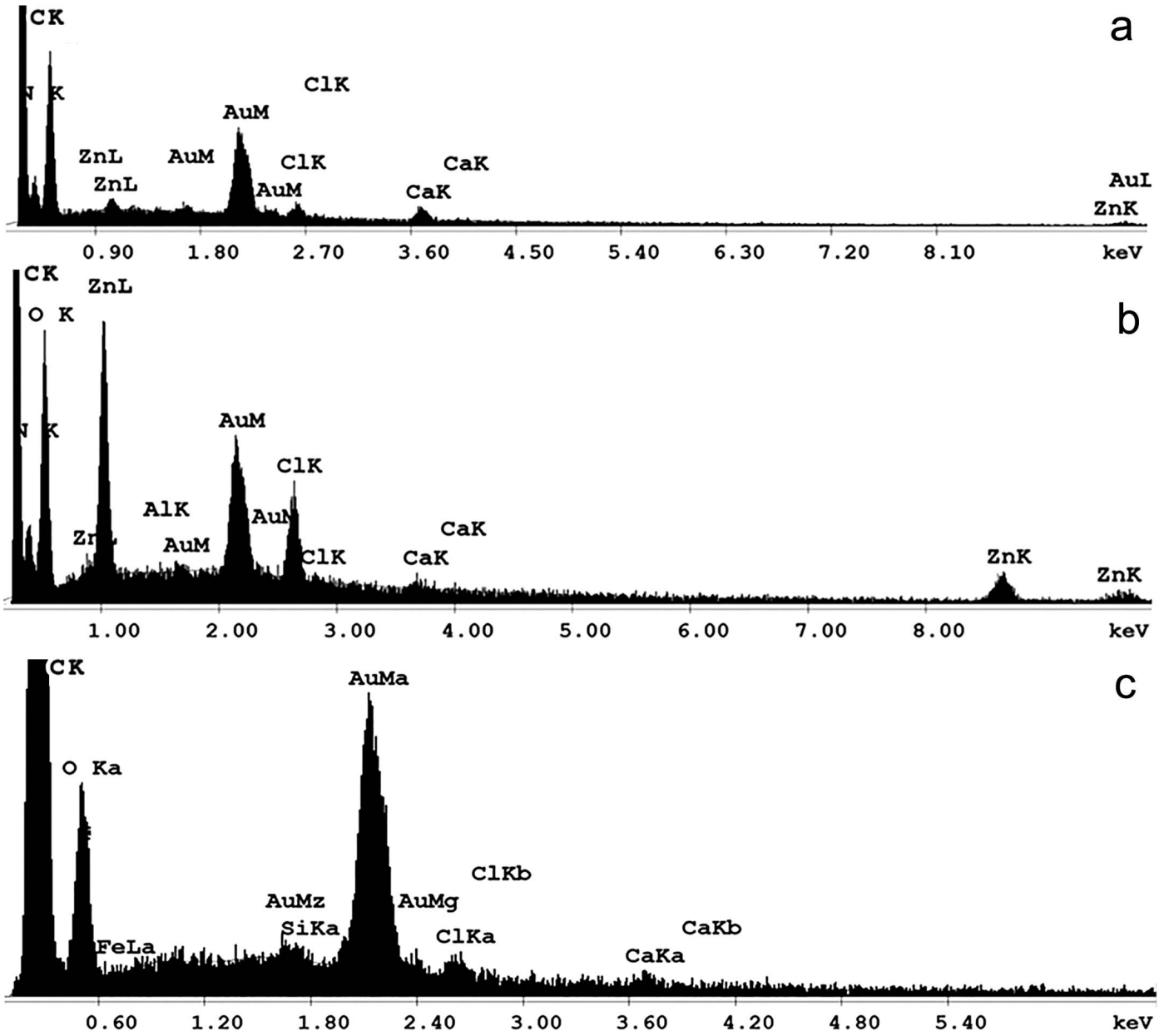

Figure 3.—EDS spectrograms of juvenile exoskeleton of *Phrynus marginemaculatus*. a. pedipalp tibia. b. Pedipalp tarsus. c. Tarsal claw. Valence shell energies (K, L, M) follow abbreviations of different chemical elements. See text for additional explanations.

On the prosoma, scans included ocular tubercles, and up to three scans at random locations (Figs. 1b, 4a). The chelicerae were examined in proximal, medial and distal areas of the basal article, distal article (fang) and teeth, three scans per area (Figs. 1c, 4b,c). Depending on the scan accessibility, no more than three teeth from each cheliceral article were examined. Pedipalp tibia analyses incorporated proximal, medial and distal areas of primary and secondary spines, spikes, and three random locations on the tibial base (Figs. 1b, 4d). Pedipalp tarsus scans included proximal, medial and distal areas of basitarsus, distitarsus (including the cleaning organ), and primary spines (Figs. 1d,e 4d). Walking leg tarsal claws were analyzed in proximal, medial and distal areas, two scans per area (Figs. 1f, 4e). Additionally, setae and fringe hairs were scanned in proximal and distal areas.

RESULTS

The scanning results presented here are only related to the uppermost layers of a whip spider's exoskeleton. The detection limit in EDS analyses is 0.1 weight percentage (% wt.), with an accuracy of ± 1 standard deviation (SD) (Chandler & Roberson 2009). While we provide this level of detection accuracy in our tables (Tables 1, 2, 3), we have chosen to use 1.0 % wt. as the standard for "presence" of an element to maintain consistency with previous publications, which also

Table 1.—Weight percentages of trace elements revealed by EDS analyses of select regions of the exoskeleton of juvenile *Phrynus marginemaculatus*. Weight percentages represent the averages (± 1 SD) of three scans rounded to two decimal places. Only weight percentages above 1.0 % of major trace elements are shown for ease of comparison to Gallant et al. (2016) and Gallant & Hochberg (2017). Regions where weight percentages were less than 1.0 % are indicated by "–".

	Body regions				
Elements	Prosoma	Chelicerae	Pedipalp tarsi	Pedipalp tibiae	Leg tarsal claws
Na	–	–	–	–	–
K	–	–	–	–	–
Ca	–	–	2.6 ± 2.9	5.5 ± 7.6	–
Mn	–	–	–	–	–
Zn	–	–	5.4 ± 6.5	2.5 ± 6.0	–

used 1.0 % because of the high SDs and noise levels (e.g., Gallant et al. 2016; Gallant & Hochberg 2017).

Six specimens were examined and included three juveniles (Fig. 1a: sacrificed 2nd instars) and three adults (two molts and one sacrificed). The following elements were detected: aluminum (Al), calcium (Ca), carbon (C), chlorine (Cl), fluorine (F), iron (Fe), magnesium (Mg), manganese (Mn), nickel (Ni), nitrogen (N), oxygen (O), potassium (K), sodium (Na), sulfur (S), silicon (Si), and zinc (Zn). Only elements close to or above noise levels (1% wt.) are labeled in the EDS spectra (Figs. 2,3,5,6). Since carbon, nitrogen and oxygen constitute the main elements that make up chitin and proteins, they are excluded from the results below. Magnesium, iron, nickel, aluminum, fluorine, sulfur, and silicon were only detected in a few areas and never averaged above 1 % wt. Six elements were present – Ca, Cl, Fe, Mn, Na, and Zn – at different levels depending on the region of examination as well as the developmental stage of the specimen.

Importantly, NaK and ZnL X-ray lines have similar energies (overlapping peaks) in EDS scans (Newbury 2009). Therefore, it was necessary to run a control with zinc oxide (ZnO) powder to better understand how to separate their shell energies and quantify the relative amounts of each element (Figs. 2a, b). Ten control scans of ZnO powder were performed and ZnL/ZnK ratios with SD calculated – the average ZnL/ZnK ratio was 3.69 ± 0.99%. The controls allowed the confirmation of the presence or absence of zinc in relation to sodium. Whenever the ZnL/ZnK ratio in the specimen scans was higher than 4.70, that confirmed the presence of Na (the ZnL/ZnK ratio was never below 2.70).

Juveniles (Figs. 1–3; Tables 1, 2).—A total of seven trace elements were detected in juveniles: Al, Ca, Cl, Fe, K, Na, and Zn. Not all elements averaged above 1% wt., and many had uneven distributions across the exoskeleton.

Prosoma: The surface of the prosoma was slightly wavy with uniformly scattered tubercles (Figs. 1a, b). Six trace elements were detected, but none averaged above 1 % wt: Ca (0.56 ± 0.41 %), Cl (0.54 ± 0.31 %), Fe (0.21 ± 0.32 %), K (0.34 ± 0.21 %), Na (0.31 ± 0.06 %), and Zn (0.47 ± 0.66 %). Zinc was only above 1 % wt in the area of the medial ocular tubercles (Fig. 2c).

Chelicerae: The distal article (fang) was half the size of the basal article. The basal article contained three teeth; the distal tooth was the longest, and the proximal tooth was bicuspidate with a longer upper cusp. The dorsolateral sides of the distal article and ventral part of the basal article were covered in setae (Fig. 1c). Five trace elements were detected but none were present above 1 % wt: Ca (0.48 ± 0.32 %), Cl (0.54 ± 0.22 %), K (0.23 ± 0.07 %, Na (0.45 ± 0.11 %), Zn (0.25 ± 0.08 %) (Fig. 2d). Calcium was close to 1 % wt on the cheliceral teeth; however, it never exceeded 1 %.

Pedipalp tibia: The tibia contained five primary dorsal spines, of which the third and the fifth were smaller than the second and third (Fig. 1b). Six trace elements were detected (Fig. 3a; Table 2): Al (0.18 ± 0.56 %), Ca (5.48 ± 7.61 %), Cl (2.62 ± 3.81 %), K (0.71 ± 1.41 %), Na (0.55 ± 0.31 %), and Zn (2.49 ± 5.99 %) (Fig. 3a). Only Ca, Cl, and Zn were present above 1 % wt. Calcium was present throughout entire spines (Table 2), with higher values on the first and third spine. Chlorine occurred in the distal and medial areas of the spines, while zinc was only present in the distal areas. Additionally, K was above 1 % in the medial and proximal areas of the tibiae (Table 2), even though its average value was below 1 % wt.

Pedipalp tarsus: The tarsus consisted of basitarsus and distitarsus. Basitarsus had four spines, two on each side (Figs. 1d, e). Distitarsus was short and wide at the base and contained a cleaning organ surrounded by tiny setae (Fig. 1e). Both articles were sparsely covered with long setae. Seven trace elements were detected: Ca (2.59 ± 2.85 %), Cl (1.59 ± 1.19 %), Fe (0.12 ± 0.38 %), Mg (0.07 ± 0.13 %), Na (0.73 ± 0.86 %), K (0.29 ± 0.51 %), and Zn (5.35 ± 6.51 %) (Fig. 3b;

Table 2.—The presence of trace elements in select regions of juvenile *Phyrunus marginemaculatus*. A detection limit of > 1.0 % is used as the standard for presence of an element in a specific location; however, the average wt. percentage for that element might be < 1.0 % (see text). Abbreviations: +, present; –, absent; BA, basal article; D, distal area; DA, distal article; M, medial area; OT, ocular tubercle; P, proximal area.

	Prosoma		Chelicerae						Pedipalps						Leg claws		
			DA			BA			Tarsus			Tibia					
	OT	Base	D	M	P	D	M	P	D	M	P	D	M	P	D	M	P
Na	–	–	–	–	–	–	–	–	+	–	–	–	–	–	–	–	–
K	–	–	–	–	–	–	–	–	–	–	–	–	+	+	–	–	–
Ca	–	–	–	–	–	–	–	–	+	+	+	+	+	+	–	–	–
Mn	–	–	–	–	–	–	–	–	–	–	–	–	–	–	–	–	–
Zn	+	–	–	–	–	–	–	–	+	+	–	+	–	–	–	–	–
Cl	–	–	–	–	–	–	–	–	+	+	–	+	+	–	–	–	–

Table 3.—Weight percentages of trace elements revealed by EDS analyses of select regions of the exoskeleton of adult *Phrynus marginemaculatus*. Weight percentages represent the averages (± 1 SD) of three scans rounded to two decimal places. Only weight percentages above 1.0 % of major trace elements are shown for ease of comparison to Gallant et al. (2016) and Gallant & Hochberg (2017). Regions where weight percentages were less than 1.0 % are indicated by "–".

Elements (average % wt + SD)	Body regions				
	Prosoma	Chelicerae	Pedipalp tarsi	Pedipalp tibiae	Leg tarsal claws
Na	–	1.7 ± 2.6	–	1.9 ± 2.9	–
K	–	1.0 ± 1.2	1.0 ± 2.4	–	1.0 ± 1.3
Ca	2.5 ± 1.1	5.9 ± 8.8	3.6 ± 7.7	6.1 ± 4.4	2.4 ± 3.9
Mn	–	–	1.9 ± 3.9	–	–
Zn	1.2 ± 1.0	11.8 ± 18.9	6.6 ± 10.6	1.2 ± 0.8	5.8 ± 7.1
Cl	–	2.2 ± 2.7	2.0 ± 3.1	6.6 ± 0.9	3.5 ± 4.7

Table 2). Calcium was prevalent throughout the tarsal articles, with the highest amounts in the medial areas of the spines and distitarsal claw (Table 2). Zinc was only present in the distal areas of the spines and distal claw, while Chlorine was detected in the distal and medial areas of the tarsal articles. Sodium was above 1 % wt only in the distal areas of the distitarsus.

Leg tarsal claws: Claws were striated with acute tips. Hairs were present around the claws (Fig. 1f). Three trace elements were present: Ca (0.66 ± 0.24 %), Cl (0.55 ± 0.39 %) and Zn (0.59± 0.21 %) (Fig. 3c; Table 2).

Adult (Figs. 4–7; Tables 3, 4).—A total of 11 trace elements were detected in adults: Al, Ca, Cl, Fe, K, Mg, Mn, Na, S, Si, and Zn. Not all elements averaged above 1% wt., and many had uneven distributions across the exoskeleton.

Prosoma: The surface of the prosoma was covered with tubercles of different sizes, with larger tubercles dominating the distal areas (Fig. 4a). Seven trace elements were detected: Al (0.35 ± 0.67 %), Ca (2.5 ± 1.06 %), Cl (0.61 ± 0.20 %), K (0.85 ± 0.54 %), Mg (0.23 ± 0.16 %), Na (0.60 ± 0.35 %), and Zn (1.16 ± 1.03 %) (Fig. 5a; Tables 3, 4). Only Ca and Zn averaged above 1 %. Potassium (up to 1.67 %) and chlorine (up to 1.32 %) were present above 1 % wt in the central areas of the carapace, but their averages were < 1%. Additionally, these areas had higher values of Ca (up to 5.95 %) and Zn (up to 2.87 %) (Tables 3, 4). Ocular tubercles did not show higher level of enrichment.

Chelicerae: The fang was half the length of the basal article and highly curved (Figs. 4b, c). The basal article contained three teeth; the distal tooth was the longest, and the proximal tooth was bicuspidate with a longer upper cusp. The ventral side of the basal article was covered with fringe setae (Fig. 4c). The distal article was covered with fringe setae dorsally in the medial area and ventrolaterally in the proximal area. Six trace elements were detected: Ca (5.93 ± 8.83 %), Cl (2.22 ± 2.70 %), K (0.97 ± 1.17 %), Mg (0.14 ± 0.18 %), Na (1.74 ± 2.62 %), and Zn (11.84 ± 18.86 %) (Fig. 5c). Only four trace elements had average weight percentages above 1 %. Chlorine, sodium and zinc were present in distal and medial areas of the fang and teeth, while Ca was present in the medial and proximal areas.

Pedipalp tibia: The tibia had five dorsal primary spines (Fig. 4d). The tibial base was completely covered with tubercles of different sizes. Six trace elements were detected: Ca (6.15 ± 4.42 %), Cl (6.59 ± 0.85 %), K (0.84 ± 0.25 %), Mn (0.67 ± 0.18 %), Na (1.88 ± 2.94 %), and Zn (1.15 ± 0.76 %). (Fig. 6a). The Zn (up to 35 % wt) and Na (up to 5.27 % wt) were high in the distal areas of the primary spines, while Ca (up to 10.19 % wt) and Cl (up to 7.53 % wt) were high throughout the spines. Manganese was high at the distal and medial areas of the secondary spines, but its average was below 1 %. Potassium was not present above 1 % (Fig. 6a).

Pedipalp tarsus: The basitarsus contained two spines on each lateral side (Fig. 4d). Eight trace elements were present: Ca (3.62 ± 7.71 %), Cl (1.99 ± 3.11 %), K (0.98 ± 2.39 %), Mg (0.14 ± 0.18 %), Mn (1.91 ± 3.94 %), Na (0.90 ± 1.37 %), S (0.46 ± 1.96 %), and Zn (6.55 ± 10.58 %). However, only Ca, Cl, Mn, and Zn were present above 1 % (Fig. 7a). All eight trace elements were present in the medial area, while only Ca, Cl and Zn were detected in the proximal area (Table 4). Sulphur was detected on only one spot of the examined area; hence it might represent an artifact.

Leg tarsal claws: The claws were sharp with striated surfaces (Fig. 4e). Ten trace elements were present: Al (0.24 ± 0.56 %), Ca (2.40 ± 3.89 %), Cl (3.51 ± 4.69 %), Fe (0.23 ± 0.81 %), K (0.97 ± 1.28 %), Mg (0.15 ± 0.21 %), Mn (0.23 ± 0.50 %), Na (0.79 ± 0.28 %), Si (0.24 ± 0.83 %) and Zn (5.79 ± 7.05 %) (Fig. 7c). Potassium values averaged close to 1 % wt., but in the medial area they were above 1 % (Table 4). Zinc was present only distally, while calcium was present in the distal and medial areas (Table 4). Chlorine was detected in the medial and proximal areas of the claws.

Adult exuviae (Figs. 5–7; Tables 5, 6).—A total of ten trace elements were detected in adults: Al, Ca, Cl, Fe, K, Mg, Mn, Na, Ni, and Zn. Not all elements averaged above 1% wt., and many had uneven distributions across the exoskeleton.

Prosoma: Eight trace elements were present: Al (0.36 ± 0.49 %), Ca (2.10 ± 1.56 %), Cl (0.92 ± 0.46 %), Fe (0.12 ± 0.32 %), K (0.92 ± 0.46 %), Mg (0.29 ± 0.15 %), Na (0.51 ± 0.37 %), and Zn (1.03 ± 1.07 %) (Fig. 5b; Tables 5, 6). Only Ca and Zn had averages above 1 %.

Chelicerae: Six trace elements were present: Ca (8.32 ± 11.86 %), Cl (0.65 ± 0.41 %), Mg (0.19 ± 0.20 %), Mn (0.10 ± 0.44 %), Na (0.45 ± 0.34 %) and Zn (8.92 ± 8.14 %) (Fig. 5d). Only Ca and Zn averaged above 1% wt. Both were present in the medial region of both articles, while Zn was absent from the proximal region (Table 6).

Pedipalp tibia: Nine trace elements were present: Al (0.26 ± 0.95 %), Ca (2.13 ± 2.98 %), Cl (1.01 ± 1.26 %), Fe (0.32 ± 0.84 %), K (0.11 ± 0.23 %), Mg (0.16 ± 0.19 %), Na (0.59 ± 0.34 %), Ni (0.14 ± 0.51 %) and Zn (2.13 ± 2.41 %) (Fig. 6b). Chlorine and Zn were present distally and medially, while Ca

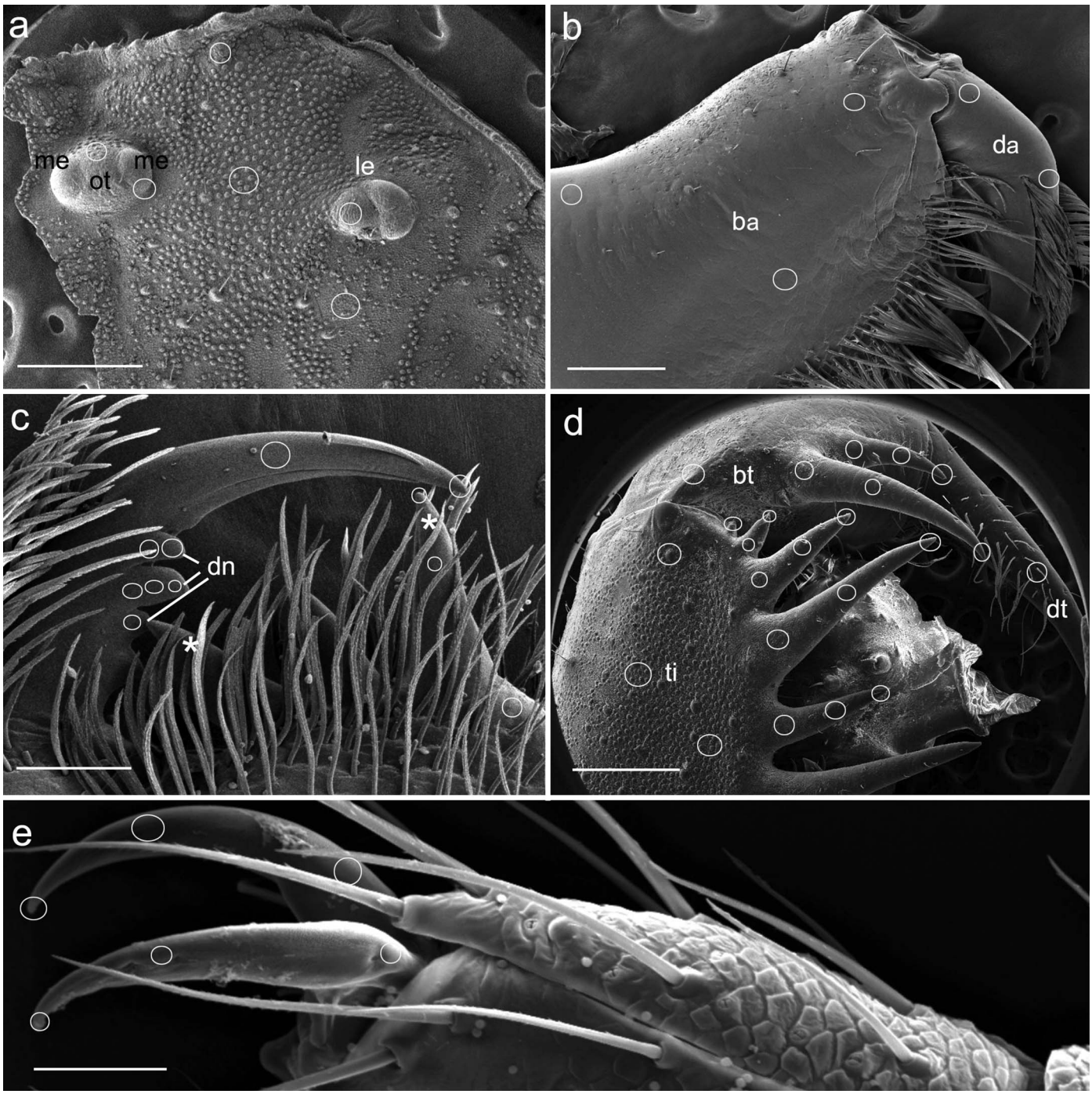

Figure 4.—Adult *Phrynus marginemaculatus*. Scanning electron micrographs of regions scanned for elemental enrichment. Ovals represent approximate regions of EDS data collection. See text for specific locations a. Closeup of anterior end of prosoma carapace. b. Chelicera. c. Fang and dentition of chelicera. d. Pedipalp removed from specimen. e. Tarsal claws. Abbreviations: * dentition of basal article; ba, basal article of chelicera; bt, basitarsus of pedipalp; da, distal article of chelicera; dn, dentition of chelicera; dt, distitarsus of pedipalp; le, lateral eye; me, medial eye; ot, ocular tubercle. ti, pedipalp tibia. Scale bars: a, 400 μm; b, 200 μm; c, 50 μm; d, 350 μm; e, 40 μm.

was present medially and proximally (Table 6). Aluminum and iron were only detected on one specimen on the second dorsal spine (with values above 2 %) and possibly represent an artifact.

Pedipalp tarsus: Eight trace element were present: Al (0.13 ± 0.40 %), Cl (0.87 ± 1.03 %), Ca (6.24 ± 7.06 %), K (0.32 ± 0.91 %), Mg (0.14 ± 0.19 %), Mn (2.57 ± 3.89 %), Na (0.48 ± 1.12 %), and Zn (0.25 ± 0.75 %) (Fig. 7b). Only Ca and Mn (2.57 ± 3.88 %) averaged above 1% and both were present in the distal areas of the molted pedipalp tarsi. In the medial area, the molt had Ca, Mn, and Zn. Other than Ca, no

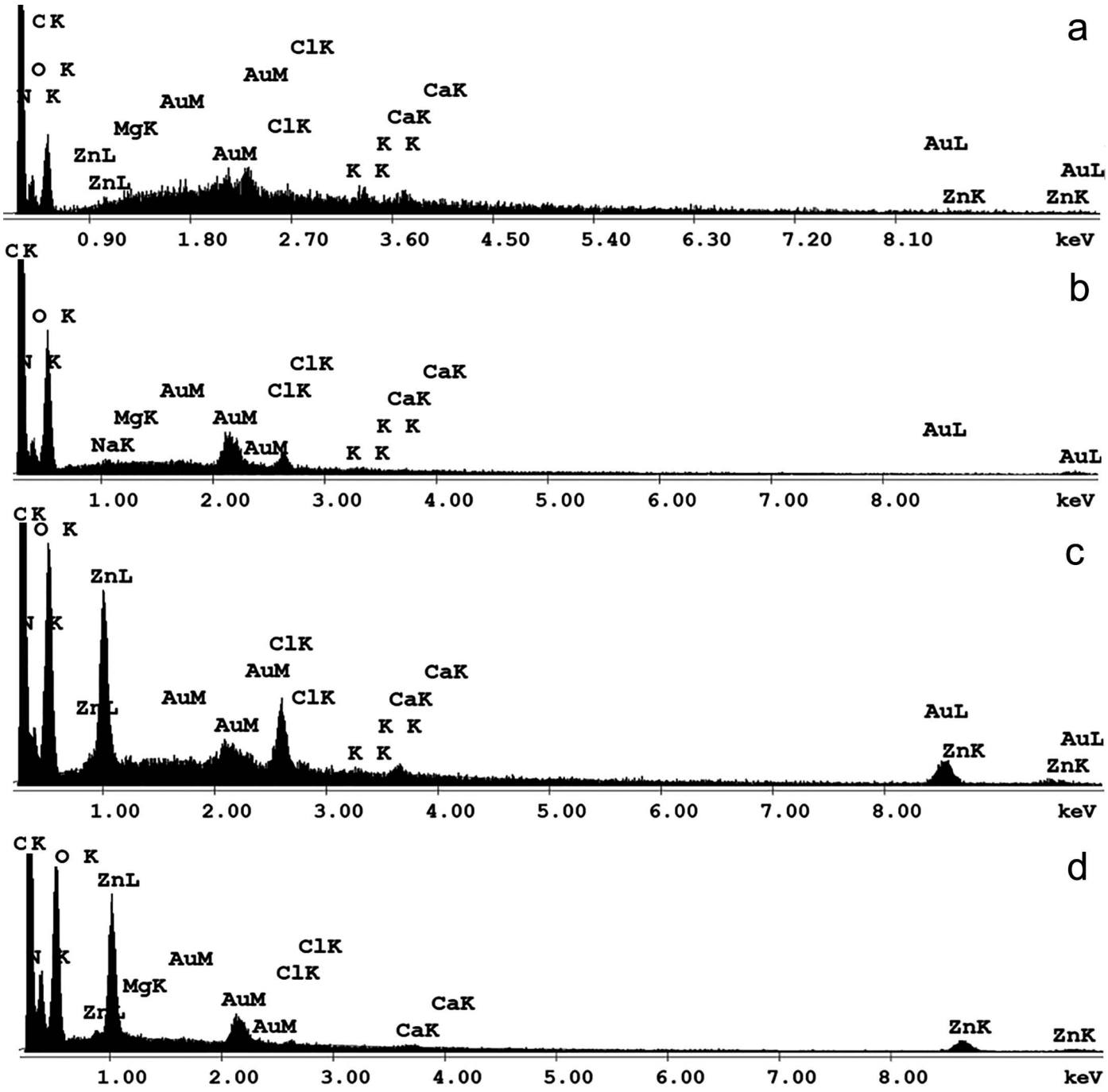

Figure 5.—EDS spectrograms of select regions of sacrificed adult and exuviae of *Phrynus marginemaculatus*. a. EDS spectrum of prosoma. b. EDS spectrum of prosoma exuviae. c. EDS spectrum of chelicera. d. EDS spectrum of chelicera exuviae. X–axis represents excitation energy of the emitted X-rays (in keV); Y–axis represents the relative X-ray line intensities. Valence shell energies (K, L, M) follow abbreviations of different chemical elements. See text for additional explanations.

element was detected on the proximal area of the molt pedipalp tarsi (Table 6).

Leg tarsal claws: Five trace elements were present: Ca (0.29 ± 0.29 %), Cl (0.64 ± 1.10 %), K (0.98 ± 2.39 %), Na (2.52 ± 1.63 %) and Zn (6.00 ± 2.30 %) (Fig. 7d). Only Na and Zn were present above 1 % wt. Only Cl, Ca, and Zn were present in the distal areas of the claws (Table 6).

DISCUSSION

During the last twenty years, most amblypygid research has focused on taxonomy, physiology, and behavior, with comparatively little research on the properties of their cuticle (Wolff et al. 2015, 2016a, b; Filipov et al. 2017). Even though Amblypygi is a relatively small taxon containing species with a highly conserved morphology, there are important differences

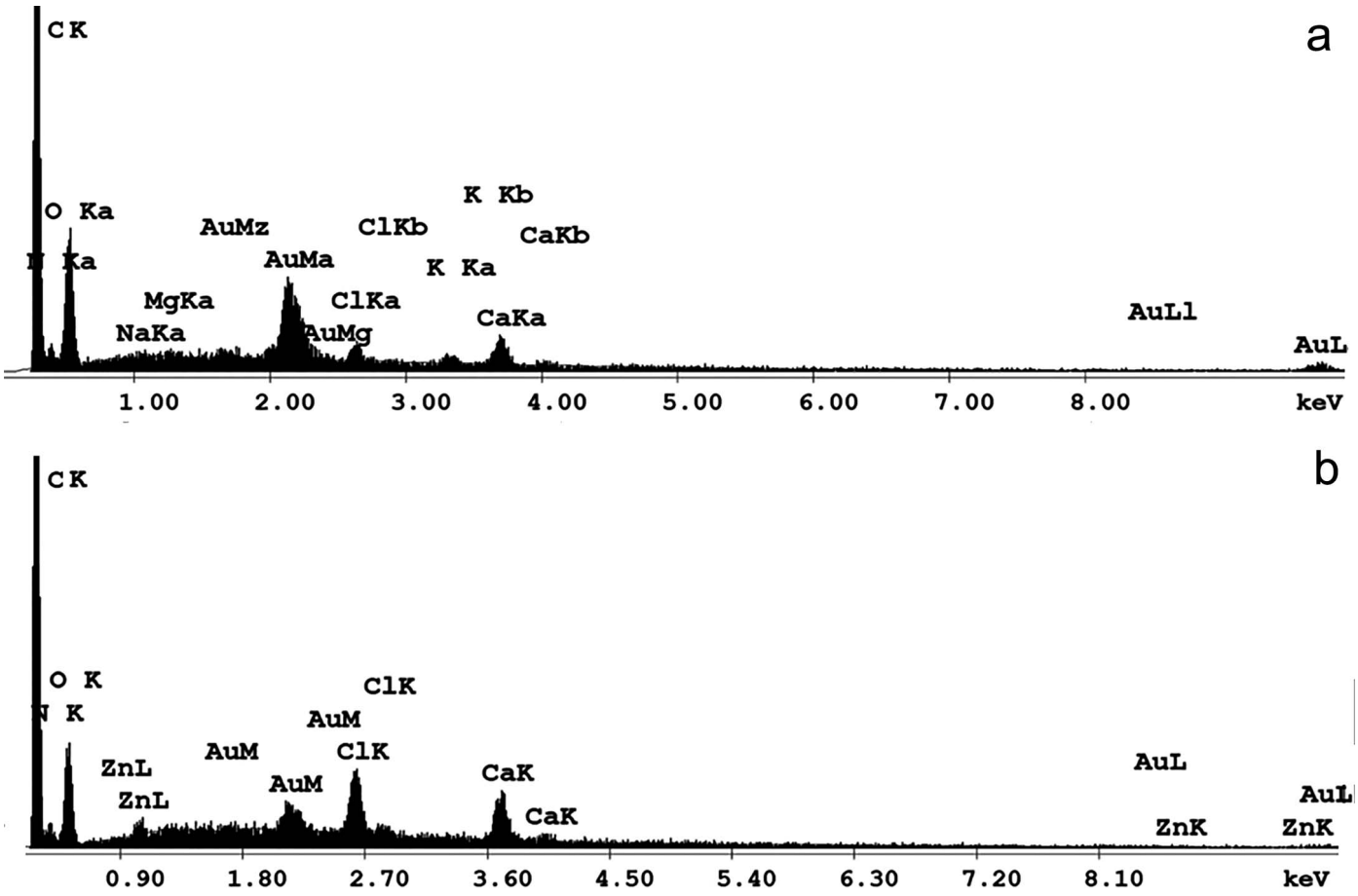

Figure 6.—EDS spectrograms of select regions of sacrificed adult and exuviae of *Phrynus marginemaculatus*. a. EDS spectrum of pedipalp tibia. b. EDS spectrogram of pedipalp tibia exuviae. X–axis represents excitation energy of the emitted X-rays (in keV); Y–axis represents the relative X-ray line intensities. Valence shell energies (K, L, M) follow abbreviations of different chemical elements. See text for additional explanations.

among species in terms of size and habitat (e.g., arid, tropical, caves, trees, under rocks) that may be reflected in the structure and composition of their exoskeletons. In this study, we chose to focus on a well-known species (*Phrynus marginemaculatus*) in order to provide a baseline for future research on intraspecific variation centered on diet or other parameters important in captive breeding (McMonigle 2013), as well as for comparisons to other species from a variety of different environments.

Elemental analyses were conducted at 17 locations on all specimens and focused strictly on the outside of the exoskeleton, which is known to possess a secreted cerotegument that is hydrophobic (Wolff et al. 2016a, b) and may function as a substrate for fungal growth (Gibbons et al. 2019). For these reasons, we cannot be certain that the elements detected in our analyses (a total of 13 trace elements in juveniles, adults, and adult exuviae (Tables 2,4,6)) are all native to the whip spider exoskeleton. Regardless, our SEM observations did not detect any obvious fungal growth in our specimens (see Gibbons et al. 2019; fig. 1), so we are confident that most of our elemental data comes from the hardened exoskeleton only.

Our focus on the prosoma, chelicerae, pedipalps, and tarsal claws is based on the results of previous studies of the arthropod cuticle that showed the occurrence of transition and alkaline earth metal elements in these regions (Schofield 1990; Fawke et al. 1997; Schofield et al. 2003; Cutler & McCutchen 2006; Gallant et al. 2016; Gallant & Hochberg 2017; Politi et al. 2017; Tadayon et al. 2020). The chelicerae, pedipalps and tarsal claws are all exposed to frequent mechanical stress during feeding, defense, and locomotion, and need to be structurally reinforced; other regions such as the prosoma may also require reinforcement if attacks from other arthropods come from above. Even though these structures (whole appendages and the prosoma) can be renewed during molting, adults do not molt frequently, and for larger arthropods, these structures need to last a minimum of one year, which is the time between molts (Weygoldt 2000; Bar-On et al. 2014). The antenniform appendages (modified 1st walking legs) were not analyzed in this study because they are not used in prey handling nor do they appear to contact the environment with any significant force (personal observations).

Of the trace elements detected in the whip spider cuticle, zinc is the most common metal ion and one that is regularly detected in arachnid exoskeletons, where it is hypothesized to harden regions that function in prey handling and have direct contact with the substrate (Schofield 1990, 2001; Schofield et al. 2003; Cutler & McCutchen 2006; Politi et al. 2017). As

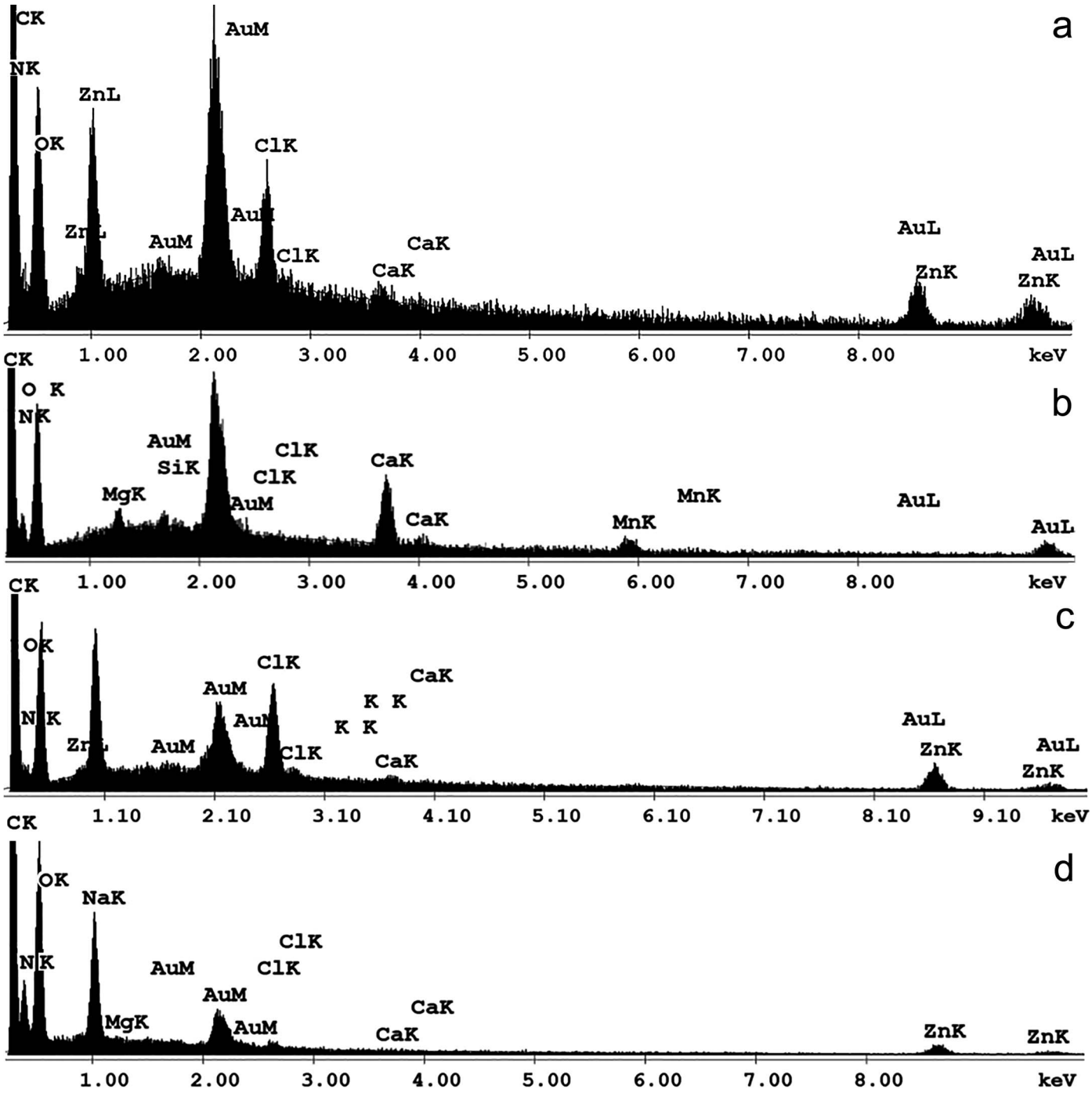

Figure 7.—EDS spectrograms of select regions of sacrificed adult and exuviae of *Phrynus marginemaculatus*. a. EDS spectrogram of pedipalp tarsus. b. EDS spectrum of pedipalp tarsus exuviae. c. EDS spectrum of tarsal claw. d. EDS spectrum of tarsal claw exuviae. X–axis represents excitation energy of the emitted X-rays (in keV); Y–axis represents the relative X-ray line intensities. Valence shell energies (K, L, M) follow abbreviations of different chemical elements. See text for additional explanations.

whip spiders are known predators of insects and other arthropods (Weygoldt 2000), we reasoned that Zn might be a common trace element in the chelicerae and pedipalps of whip spiders. Results revealed that this metal ion had a surprisingly restricted distribution in juvenile whip spiders (prosoma, pedipalps) but was present throughout the exoskeleton (prosoma, pedipalps, chelicerae, tarsal claws) of the adult amblypygid including the two exuviae. This suggests that Zn may only be actively incorporated into the whip spider exoskeleton at select locations (e.g., chelicerae, tarsal claws) after a period of time (e.g., 3rd instar or later). The functional significance of this is unknown but may be related to a change in diet as whip spiders mature, i.e., they feed on successively larger prey that may have thicker exoskeletons (e.g., crickets).

Zinc was commonly found in the regions of the exoskeleton that also contained sodium and chlorine. Sodium had its

Table 4.—The presence of trace elements in select regions of an adult *Phrynus marginemaculatus*. A detection limit of > 1.0 % is used as the standard for presence of an element in a specific location; however, the average wt. percentage for that element might be < 1.0 % (see text). Abbreviations: +, present; –, absent; BA, basal article; D, distal area; DA, distal article; M, medial area; OT, ocular tubercle; P, proximal area.

	Prosoma		Chelicerae						Pedipalps						Leg claws		
			DA			BA			Tarsus			Tibia					
	OT	Base	D	M	P	D	M	P	D	M	P	D	M	P	D	M	P
Na	–	–	+	+	–	+	+	–	–	+	–	+	–	–	+	–	–
K	–	+	–	+	+	–	+	–	–	+	–	–	–	–	–	+	–
Ca	–	+	–	+	+	–	+	+	–	+	+	+	+	+	+	+	–
Mn	–	–	–	–	–	–	–	–	+	+	–	–	+	–	–	–	–
Zn	–	+	+	+	–	+	+	–	–	+	+	+	–	–	+	–	–
Cl	–	–	+	+	–	+	+	–	–	+	+	+	+	+	–	+	+

highest values when Zn values were exceptionally high, and as mentioned previously, NaK shell energy overlaps with the ZnL shell energy. Hence, the Na amounts could not be determined accurately, nor with certainty, when Zn amounts were also high. For this reason, we hesitate to speculate on the functional significance of Na in the whip spider exoskeleton. The presence of Cl could potentially be explained through the formation of zinc-chlorides (Schofield 1990, 2001; Schofield et al. 2003). This Zn-Cl correlation has been observed in other arthropods, such as insects and non-buthid scorpions, where amounts of Zn frequently matched the amounts of Cl (Hillerton & Vincent 1982; Schofield 2001; Schofield et al. 2003). In the current study, however, the weight percentages of Cl were frequently much lower than Zn, which runs counter to the hypothesis of zinc chloride formation in the exoskeleton. Nonetheless, it is highly probable that the presence of Cl indicates the presence of Zn (Schofield 2001; Schofield et al. 2003; Cribb et al. 2007; Gallant & Hochberg 2017) and vice versa. It is known that Cl ions bind to Zn ions during protein transport in different biochemical processes, and that they participate in Zn stabilization and coordination within the protein matrix (Politi et al. 2017). In the jaws of the clam worm *Nereis virens* Sars, 1835, tyrosine and histidine can become chlorinated, which together with Zn form complexes that enhance the stiffness of the jaws (Lichtenegger et al. 2003; Birkedal et al. 2006; Broomell et al. 2006; Politi et al., 2017). How Zn and Cl interact in the arachnid cuticle remains to be elucidated, but it is not unreasonable to hypothesize that their combination leads to a hardening of the cuticle in select locations.

Calcium was present in all examined whip spiders. In juveniles, it only exceeded 1% weight in the pedipalps and was close to 1% in the chelicerae. In the adult exoskeleton, it exceeded 1% in all examined areas, including the exuviae; more specifically, Ca was present in the middle areas of cheliceral fangs, bases of cheliceral teeth, tarsal and tibial primary spines, and walking leg tarsal claws. The highest amounts of Ca in adults were detected in the chelicerae, where Zn was also present. Based on previous studies, Ca is rarely abundant in the exoskeleton of any group of arachnids other than the Thelyphonida and Araneae (Schofield et al. 2003; Cutler & McCutchen 2006; Gallant & Hochberg 2017). In whip spiders, the chelicerae are enriched with Ca and Zn, although Zn is often present at a much higher percentage (Gallant & Hochberg 2017). The fact that Ca and Zn were discovered in the same regions in whip spiders and whip scorpions (Thelyphonida) might signify a conserved elemental profile of the group Pedipalpi (Amblypygi, Thelyphonida, Schizomida) or Tetrapulmonata (Araneae, Amblypygi, Thelyphonida, Schizomida); alternatively, the presence of both elements in the same regions could indicate independent elemental enrichments based on similarities in habitat or prey types.

What form calcium takes in the arachnid exoskeleton remains to be determined. In marine pancrustaceans such as lobsters, Ca is present as amorphous calcium phosphate (Schofield 2001; Erko et al. 2013), which is also true of some terrestrial pancrustaceans such as isopods (Huber et al. 2014) and insects (Cribb et al. 2005; Rong et al. 2019). In other species, calcium appears to form nano-crystals (Cribb et al.

Table 5.—Weight percentages of trace elements revealed by EDS analyses of select regions of the exoskeleton of two exuviae of adult *Phrynus marginemaculatus*. Weight percentages represent the averages (± 1 SD) of three scans. Only weight percentages above 1.0 % of major trace elements are shown for ease of comparison to Gallant et al. (2016) and Gallant & Hochberg (2017). Regions where weight percentages were less than 1.0 % are indicated by "–".

Elements (average % wt with SD)	Body regions				
	Prosoma	Chelicerae	Pedipalp tarsi	Pedipalp tibiae	Leg tarsal claws
Na	–	–	–	–	2.5 ± 1.6
K	–	–	–	–	–
Ca	2.1 ± 1.6	8.3 ± 11.9	6.2 ± 7.1	2.2 ± 3.0	–
Mn	–	–	2.6 ± 3.9	–	–
Zn	1.0 ± 1.1	8.9 ± 8.1	–	2.1 ± 2.4	6.0 ± 2.3
Cl	–	–	–	1.0 ± 1.3	–

Table 6.—The presence of trace elements in adult exuviae of *Phrynus marginemaculatus*. A detection limit of > 1.0 % is used as the standard for presence of an element in a specific location; however, the average wt. percentage for that element might be < 1.0 % (see text). Abbreviations: +, present; –, absent; BA, basal article; D, distal area; DA, distal article; M, medial area; OT, ocular tubercle; P, proximal area.

	Prosoma		Chelicerae						Pedipalps						Leg claws		
			DA			BA			Tarsus			Tibia					
	OT	Base	D	M	P	D	M	P	D	M	P	D	M	P	D	M	P
Na	–	–	–	–	–	–	–	–	+	–	–	+	–	–	+	–	–
K	–	+	–	–	–	–	–	–	–	+	–	–	–	–	–	–	–
Ca	–	+	–	+	+	–	+	+	+	+	+	–	+	+	–	–	–
Mn	–	–	–	–	–	–	–	–	+	+	–	–	–	–	–	–	–
Zn	–	+	+	+	–	+	+	–	–	+	–	+	+	–	+	–	–
Cl	–	–	+	+	–	+	+	–	+	–	–	+	+	–	+	–	–

2007). The absence of phosphorus in the scans of whip spiders suggests that these arachnids do not form calcium-phosphate. An ultrastructural study of the whip spider exoskeleton might therefore be useful for determining if Ca nano-particles can be detected as in the study of Cribb et al. (2005).

Manganese was only detected in the pedipalps of adult *P. marginemaculatus*. It was consistently present at the distal areas of the pedipalp tarsi, more precisely on the distitarsus and secondary spines. In spiders, Mn is present in the fangs and tarsal claws (Schofield 2005), while in scorpions, it is present in the tarsal claws and stings (Schofield et al. 2003); in species of Ricinulei, it is only present in the cheliceral teeth (Cutler & McCutchen 2006). Manganese is proposed to enhance both sturdiness and elasticity of the cuticle (Schofield 1990; Schofield et al. 2003; Gallant et al. 2016; Tadayon et al. 2020).

Other trace elements were found in the exoskeleton of *P. marginemaculatus*, but they never exceeded noise levels and we are uncertain if their presence in the result of contamination. For example, Al, Fe, and Si were detected in our specimens, but at extremely low levels. To date, Al is only known from whip scorpions (Gallant & Hochberg 2017), but at similarly low levels to those detected in the current study. The difficulty with accurately detecting Al is due to the proximity of the Kα X-ray lines (1.486 eV) to Br Lα X-ray lines (1.481 eV). Because Br is implicated in cuticular sclerotization (Schofield et al. 2009), it may seem a more reasonable candidate for incorporation into the exoskeleton. However, to be certain of the presence of Br, it is necessary to find Br LKα X-ray peaks, which we did not detect. Additionally, Br has never been detected in arachnids, and presently, is known from mostly marine pancrustaceans (e.g., Cribb et al. 2009; Schofield et al. 2009; Mekhanikova et al. 2012). In contrast, Fe is relatively common in the cuticle of some arachnids (e.g., scorpions, pseudoscorpions; Schofield 1990; Cutler & McCutchen 2006; Gallant et al. 2016). Among arachnids, Si has been detected in whip scorpions (Gallant & Hochberg 2017), but it is known from some pancrustaceans including terrestrial insects (Rong et al. 2019) and freshwater copepods (Michels & Gorb 2015; Namouva et al. 2015). Interesting, Si is hypothesized to be correlated with elasticity in plant cell walls (Emadian & Newton 1989), while Fe is hypothesized to add sturdiness (Schofield 1990; Gallant et al. 2016). It is possible that the combination of these elements enhances the durability and functionality of the spines that form the pedipalpal "catching basket" of whip spiders.

In summary, our analyses revealed the presence of numerous trace elements in the exoskeleton of *P. marginemaculatus*. These analyses were used to answer two questions.

(1) Does the exoskeleton of abrasion-prone appendages of *P. marginemaculatus* share a similar elemental profile to that of other arachnids? Our studies revealed the presence of several transition and alkaline earth metal elements in the appendages of *P. marginemaculatus*, many of which are shared with species of Araneae, Scorpiones, and Thelyphonida, among other arachnids (see references above). The discovery of Ca in the amblypygid cuticle may signify a relatively conserved elemental profile of the group Pedipalpi, or even Tetrapulmonata. Furthermore, the presence of Zn suggests that the enrichment of different mouth parts with this transition metal ion is an evolutionarily conserved feature of arthropods (e.g., Schofield 2001; Schofield et al. 2003).
(2) Are there detectable differences in elemental profiles among age groups (instars) raised in a similar environment? We did detect differences between the second instars and adults; our single adult had traces of K, Mg, Mn, Si, and S that were not detected in the juveniles. Furthermore, we note that several elements increased in weight percentage from juvenile to adult, but these results should be interpreted with caution since we used relatively few specimens and none of their exoskeletons were polished, which would otherwise provide more accurate results. Future studies should consider examining: (1) the differences between prenymphs and older instars (protonymphs) to determine if the extent of sclerotization is correlated with increased elemental enrichment in successive developmental stages (see Wolff et al. 2015) and (2) a wider range of captively-bred, similarly-sized species to minimize dietary and size-related effects.

ACKNOWLEDGMENTS

The authors are indebted to two anonymous reviewers that made invaluable suggestions to improve this manuscript. We also thank the Independent University Alumni Association at Lowell and Experiment.com for funding most of the research. The authors have no conflict of interest to declare.

LITERATURE CITED

Bar-On B, Barth FG, Fratzl P, Politi Y. 2014. Multiscale structural gradients enhance the biomechanical functionality of the spider fang. *Nature Communications* 5:3894, DOI: 10.1038/ncomms4894.

Birkedal H, Khan RK, Slack N, Broomell C, Lichtenegger HC, Zok F. et al. 2006. Halogenated veneers: protein cross-linking and halogenation in the jaws of *Nereis*, a marine worm. *Chembiochem* 7:1392–1399.

Broomell CC, Mattoni MA, Zok FW, Waite JH. 2006. Critical role of zinc in hardening of *Nereis* jaws. *Journal of Experimental Biology* 209:3219–3225.

Chandler DE, Roberson RW. 2009. Bioimaging – Current Concepts in Light and Electron Microscopy. 1st ed. Jones and Bartlett Publishers, MA, USA.

Chapin KJ, Hebets EA. 2016. The behavioral ecology of amblypygids. *Journal of Arachnology* 44:1–14.

Cribb BW, Rasch R, Barry J, Palmer CM. 2005. Distribution of calcium phosphate in the exoskeleton of larval *Exeretonevra angustifrons* Hardy (Diptera: Xylophagidae). *Arthropod Structure & Development* 34:41–48.

Cribb BW, Rathmell A, Charters R, Rasch R, Huang H, Tibbetts IR. 2009. Structure, composition and properties of naturally occurring non-calcified crustacean cuticle. *Arthropod Structure & Development* 38:173–178.

Cribb BW, Stewart A, Huang H, Truss R, Noller B, Rasch R. et al. 2007. Insect mandibles–comparative mechanical properties. *Naturwissenschaften* 95:17–23.

Cutler B, McCutchen L. 2006. Heavy metals in cuticular structures of Palpigradi, Ricinulei, and Schizomida (Arachnida). *Journal of Arachnology* 34:653–656.

Dawes CJ. 1994. Introduction to Biological Electron Microscopy: Theory and Techniques, revised edition. Ladd Research Industries, Inc. Burlington, VT, USA.

Dunlop JA. 2010. Geological history and phylogeny of Chelicerata. *Arthropod Structure and Development* 39:124–142.

Emadian SF, Newton RJ. 1989. Growth enhancement of loblolly pine (*Pinus taeda* L.) seedlings by silicon. *Journal of Plant Physiology* 134:98–103.

Erko M, Hartmann MA, Zlotnikov I, Serrano CV, Fratzl P, Politi Y. 2013. Structural and mechanical properties of the arthropod cuticle: Comparison between the fang of the spider *Cupiennius salei* and the carapace of the American lobster *Homarus americanus*. *Journal of Structural Biology* 183:172–179.

Fawke JD, McClements JG, Wyeth P. 1997. Cuticular metals – quantification and mapping by complementary techniques. *Cell Biology International* 21:675–678.

Filipov AE, Wolff JO, Seiter M, Gorb SN. 2017. Numerical simulation of colloidal self-assembly of super-hydrophobic arachnid cerotegument structures. *Journal of Theoretical Biology* 430:1–8.

Forcellado LJ, de Armas LF. 2014. Depredacion de *Centruroides gracilis* (Scorpiones : Buthidae) por *Paraphrynus cubensis* (Amblypygi : Phrynidae). *Revista Iberica de Aracnologia* 25:97–98.

Fowler-Finn KD, Hebets EA. 2006. An examination of agonistic interactions in the whip spider *Phrynus marginemaculatus* (Arachnida, Amblypygi). *Journal of Arachnology* 34:62–76.

Gallant J, Hochberg R. 2017. Elemental characterization of the exoskeleton in the whip scorpions *Mastigoproctus giganteus* and *Typopeltis dalyi* (Arachnida: Thelyphonida). *Invertebrate Biology* 136:345–359.

Gallant J, Ada E, Hochberg R. 2016. Elemental characterization of the cuticle in the marine intertidal pseudoscorpion *Halobisium occidentale*. *American Microscopical Society*, *Invertebrate Biology* 135:127–137.

Gibbons AT, Idnurm A, Seiter M, Dyer PS, Kokolski M, Goodacre SL. et al. 2019. Amblypygid-fungal interactions: the whip spider exoskeleton as a substrate for fungal growth. *Fungal Biology* 123:497–506.

Hebets E. 2002. Relating the unique sensory system of amblypygids to the ecology and behavior of *Phrynus parvulus* from Costa Rica (Arachnida, Amblypygi). *Canadian Journal of Zoology* 80:286–295.

Hebets EA, Chapman RF. 2000. Surviving the flood: plastron respiration in the non-tracheate arthropod *Phrynus marginemaculatus* (Arachnida, Amblypygi). *Journal of Insect Physiology* 46:13–19.

Hillerton JE, Vincent JF. 1982. The specific location of zinc in insect mandibles. *Journal of Experimental Biology* 101:333–336.

Huber J, Fabritius HO, Griesshaber E, Ziegler A. 2014. Function-related adaptation of ultrastructure, mineral phase distribution and mechanical properties in the incisive cuticle of mandibles of *Porcellio scaber* Latreille, 1804. *Journal of Structural Biology* 188:1–15.

Kok P. 1998. *Anolis nitens chrysopepis* (goldenscale anole) predation. *Herpetological Review* 291:41.

Krishnakumaran A. 1961. A comparative study of the arachnid cuticle II. *Zeitschrift für Vergleichende Physiologie* 44:478–486.

Krishnakumaran A. 1962. A comparative study of the cuticle in Arachnida 1. Structure and staining properties. *Zoologische Jahrbücher. Abteilung für Systematik, Geographie und Biologie der Tiere* 80:49–64.

Ladle RJ, Velander K. 2003. Fishing behavior in a giant whip spider. *Journal of Arachnology* 31:154–156.

Lehmann T, Melzer RR. 2019. The visual system of Thelyphonida (whip scorpions): support for Arachnopulmonata. *Arthropod Structure & Development* 51:23–31.

Lichtenegger HC, Schoberl T, Cross JO, Heald SM, Birkedal H, Waite JH. et al. 2003. Zinc and mechanical prowess in the jaws of *Nereis*, a marine worm. *Proceedings of National Academy of Sciences* 100:9144–9149.

Michels J, Gorb SN. 2015. Mandibular gnathobases of marine planktonic copepods–feeding tools with complex micro-and nanoscale composite architectures. *Beilstein Journal of Nanotechnology* 6:674–685.

McMonigle O. 2013. Breeding the World's Largest Living Arachnid, Amblypygid Biology, Natural History, and Captive Husbandry. Coachwhip Publications, Greenville, Ohio.

Mekhanikova IV, Andreev DS, Belozerova OY, Mikhlin YL, Lipko SV, Klimenkov IV. et al. 2012. Specific features of mandible structure and elemental composition in the polyphagous amphipod *Acanthogammarus grewingkii* endemic to Lake Baikal. *Plos One* 7:e43073.

Miranda GS, Milleri-Pinto M, Concalves-Souza T, Ponce de Leao Giupponi A, Scharff N. 2016. A new species of *Charinus* Simon 1892 from Brazil, with notes on behavior (Amblypygi, Charinidae). *ZooKeys* 621:15–36.

Naumova EY, Zaidykov IY, Tauson VL, Likhoshway YV. 2015. Features of the fine structure and Si content of the mandibular gnathobase of four freshwater species of *Epischura* (Copepoda: Calanoida). *Journal of Crustacean Biology* 35:741–746.

Newbury DE. 2009. Mistakes encountered during automatic peak identification of minor and trace constituents in electron-excited energy dispersive X-ray microanalysis. *Scanning: The Journal of Scanning Microscopes* 31:91–101.

Newbury DE, Ritchie NWM. 2013. Is scanning electron microscopy/energy dispersive x-ray spectrometry (SEM/EDS) quantitative? *Scanning: The Journal of Scanning Microscopes* 35:141–168

Nolan ED, Santibáñez-López CE, Sharma PP. 2020. Developmental gene expression as a phylogenetic data class: support for the monophyly of Arachnopulmonata. *Development Genes and Evolution* 230:137–153.

Owen JL, Cokendolpher JL. 2006. Tailless whipscorpion (*Phrynus*

longipes) feeds on Antillean crested hummingbird (*Orthorhynchus cristatus*). *Wilson Journal of Ornithology* 118:422–423.

Politi Y, Pippel E, Licuco-Massouh ACJ, Bertinetti L, Blumtritt H, Barth FG. et al. 2017. Nano-channels in the spider fang for the transport of Zn ions to cross-link His-rich proteins pre-deposited in the cuticle matrix. *Arthropod Structure & Development* 30:1–9.

Politi Y, Priewasser M, Pippel E, Zaslansky P, Hartmann J, Siegel S. et al. 2012. A spider's fang: how to design an injection needle using chitin-based composite material. *Advanced Functional Materials* 22:2519–2528.

Quintero D Jr. 1981. The amblypygid genus *Phrynus* in the Americas (Ambylypgi, Phrynidae). *Journal of Arachnology* 9:117–166.

Reagan DP. 1996. Anoline lizards. Pp. 321–345. *In* The Food Web of A Tropical Rain Forest (DP Reagan, RB Waide, eds.). University of Chicago Press, Chicago, USA.

Rong J, Lin Y, Sui Z, Wang S, Wei X, Xiao J. et al. 2019. Amorphous calcium phosphate in the pupal cuticle of *Bactrocera dorsalis* Hendel (Diptera: Tephritidae): A new discovery for reconsidering the mineralization of the insect cuticle. *Journal of Insect Physiology* 119:103964.

Santer RD, Hebets E. 2009a. Prey capture by the whip spider *Phrynus marginemaculatus* C. L. Koch. *Journal of Arachnology* 37:109–112.

Santer RD, Hebets E. 2009b. Tactile learning by a whip spider, *Phrynus marginemaculatus* C. L. Koch (Arachnida, Amblypygi). *Journal of Computational Physiology* 195:393–399.

Schofield RMS. 1990. X-ray microanalytic concentration measurements in unsectioned specimens: A technique and its application to Zn, Mn, and Fe enriched structures of organisms from three phyla. Doctoral dissertation. University of Oregon. Order Number 9117566.

Schofield RMS. 2001. Metals in cuticular structures. Pp. 235–256. *In* Scorpion Biology and Research (Brownell P, Polis G, eds.). Oxford University Press, New York.

Schofield RMS. 2005. Metal-halogen biomaterials. *American Entomologist* 51:45–47.

Schofield R, Lefevre H. 1989. High concentration of zinc in the fangs and manganese in the teeth of spiders. *Journal of Experimental Biology* 144:577–581.

Schofield RMS, Levere H, Shaffer M. 1989. Complementary microanalysis of Zn, Mn, and Fe in the chelicerae of spiders and scorpions using scanning MeV-ion and electron microprobes. *Nuclear Instruments and Methods in Physics Research, Section B: Beam Interactions with Materials and Elements (Duggan JL, Morgan IL. eds.)* 40/41:698 – 701.

Schofield RMS, Nesson MH, Richardson KA, Wyeth P. 2003. Zinc is incorporated into cuticular "tools" after ecdysis: The time course of the zinc distribution in "tools" and whole bodies of an ant and a scorpion. *Journal of Insect Phylogeny* 49:31–44.

Schofield RM, Niedbala JC, Nesson MH, Tao Y, Shokes JE, Scott RA. et al. 2009. Br-rich tips of calcified crab claws are less hard but more fracture resistant: a comparison of mineralized and heavy-element biological materials. *Journal of Structural Biology* 166:272–287.

Scholtz G, Kamenz C. 2006. The book lungs of Scorpiones and Tetrapulmonata (Chelicerata, Arachnida): evidence for homology and a single terrestrialization event of a common arachnid ancestor. *Zoology* 109:2–13.

Segovia JM, Gainett G, Willemart RH. 2020. Predatory behavior and sensory morphology of the whip spider *Charinus asturius* (Arachnida: Amblypygi). *Journal of Ethology* 38:273–280.

Seiter M, Lemell P, Gredler R, Wolff JO. 2019. Strike kinematics in the whip spider *Charon* sp. (Amblypygi: Charontidae). *Journal of Arachnology* 47:260–265.

Sharma PP, Kaluziak ST, Perez-Porro AR, Gonzalez VL, Hormiga G, Wheeler WC. et al. 2014. Phylogenetic interrogation of Arachnida reveals systemic conflicts in phylogenetic signal. *Molecular Biology & Evolution* 31:2963–2984.

Shultz JW. 2007. A phylogenetic analysis of the arachnid orders based on morphological characters. *Zoological Journal of the Linnean Society* 150:221–265.

Spence AJ, Hebets EA. 2006. Anatomy and physiology of giant neurons in the antenniform leg of the amblypygid *Phrynus marginemaculatus*. *Journal of Arachnology* 34:566–577.

Tadayon M, Younes-Metzler O, Shelef Y, Zaslansky P, Rechels A, Berner A. et al. 2020. Adaptations for wear resistance and damage resilience: micromechanics of spider cuticular "tools". *Advanced Functional Materials* 30:1–13.

Weygoldt P. 2000. Whip Spiders (Chelicerata: Amblypygi): Their Biology, Morphology and Systematics. Apollo Books, Stenstrup, Denmark.

Wolff JO, Seiter M, Gorb SN. 2015. Functional anatomy of the pretarsus on whip spiders (Arachnida, Amblypygi). *Arthropod Structure & Development* 44:524–540.

Wolff JO, Seiter M, Gorb SN. 2016a. The water-repellent cerotegument of whip-spiders (Arachnida: Amblypygi). *Arthropod Structure & Development* 46:116–129.

Wolff JO, Seiter M, Gorb SN. 2016b. Whip spiders (Amblypygi) become water-repellent by a colloidal secretion that self-assembles into hierarchical microstructures. *Zoological Letters* 2:23–33.

Manuscript received 3 June 2020, revised 6 January 2021.